Appl. Phys. B 74 [Suppl.], S291–S294 (2002)
DOI: 10.1007/s00340-002-0895-7
Applied Physics B
Lasers and Optics

M. SHIBATA[1]
M. HIRASAWA[1]
N. NAKAGAWA[1]
R. MORITA[1,✉]
A. SUGURO[2]
H. SHIGEKAWA[3]
M. YAMASHITA[1]

Experimental demonstration of phase-dispersion compensation for ultra-broadband femtosecond optical pulses generated by induced-phase modulation

[1] Department of Applied Physics, Hokkaido University and Core Research for Evolutional Science and Technology, Japan, Science and Technology Corporation, Kita-13, Nishi-8, Kita-ku, Sapporo 060-8628, Japan
[2] Display Development, Technical Research Laboratory, Citizen Watch Co. Ltd., 840 Shimotomi, Tokorozawa 359-0001, Japan
[3] Institute of Applied Physics, University of Tsukuba and Core Research for Evolutional Science and Technology, Japan Science and Technology Corporation, 1-1-1 Tennodai, Tsukuba 305-8573, Japan

Received: 19 September 2001/
Revised version: 17 November 2001
Published online: 5 July 2002 •

ABSTRACT Spectrally resolved autocorrelation traces of ultra-broadband (730 to 1250 nm) pulses generated by dispersive induced-phase modulation (IPM) and self-phase modulation in a single-mode fused-silica fiber were measured. From these measurements, effective discontinuities in group delay and group-delay dispersion in the overlapping spectral region of two input pulses owing to the IPM effect were found. Not only conventional nonlinear-chirp compensation, but also frequency-independent group-delay adjustment, both of which are essential for pulse compression of ultra-broadband femtosecond pulses generated by IPM, were experimentally demonstrated using a pulse shaper with a spatial light-phase modulator of 648 pixels.

PACS 42.65.Re; 42.65.Ky; 42.81.Qb

1 Introduction

In order to generate extremely ultra-short optical pulses such as monocycle pulses, intensive spectral broadening of pulses and compensation of complicated phase dispersion are key technologies. In 1996, we proposed the utilization of induced-phase modulation (IPM) based on nonlinear co-propagation of two or more different-color femtosecond pulses with a carrier-phase locking in a single-mode (SM) fiber for spectral broadening exceeding one octave, and the utilization of a 4-f pulse shaper with a spatial light-phase modulator (SLM) for its phase-dispersion compensation [1–3]. Later, ultra-broadband pulse generation using the IPM effect for a conventional SM fused-silica fiber (480 to 900 nm) [4] and for a SM gas-filled hollow fiber (300 to 1000 nm) [5] have been experimentally demonstrated. Moreover, the capability of the SLM pulse shaper for ultra-broadband phase-dispersion compensation has been demonstrated on the basis of the experimental generation of sub-5-fs pulses for the self-phase-modulated fiber output [6–9]. To broaden the spectrum, the IPM technique has the following advantages over self-phase modulation (SPM) using a one-color femtosecond pulse: the phase modulation efficiency is two times larger, and the output electric fields with different central wavelengths are constructively synthesized in the spectral region. However, phase-dispersion compensation of IPM-broadened pulses has not been performed owing to the complexity of its spectral phase behavior. In this paper, we experimentally demonstrate that a SLM pulse shaper enables us to compensate for the complicated phase dispersion due to the IPM effect in a SM fused-silica fiber.

2 Experimental setup and results

2.1 *Experimental setup*

The experimental setup we used is shown in Fig. 1. A SM fused-silica fiber (F-SPV, Newport) with a 2.7-µm core diameter was employed as a medium for dispersive IPM and SPM effects [4]. The two input pulses into the fiber origi-

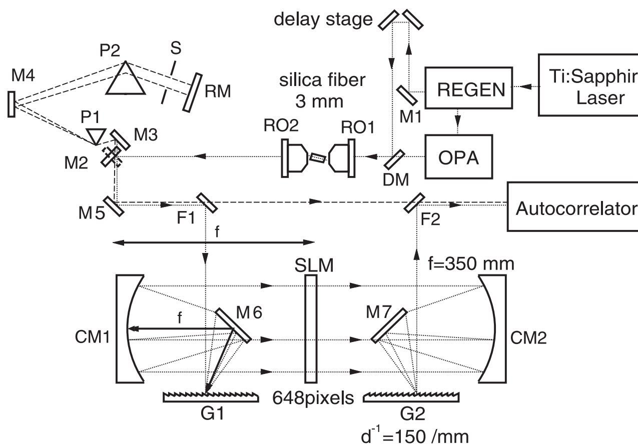

FIGURE 1 Experimental setup for spectrally resolved autocorrelation (*dashed line*) and novel phase-dispersion compensation (*solid line*) of ultra-broadband femtosecond optical pulses generated by induced- and self-phase modulations. M1–M7: plane mirrors, DM: dichroic mirror (M2 is rotated by 90° when spectrally resolved measurements are performed), F1, F2: flip mirrors, RO1, RO2: reflective objectives, P1, P2: prisms, S: slit, RM: roof mirror, G1, G2: gratings, CM1, CM2: concave mirrors, SLM: spatial light-phase modulator

✉ Fax: +81-11/706-6706, E-mail: morita@eng.hokudai.ac.jp

nated from the same light source. One pulse (the fundamental pulse) was generated by a Ti:sapphire regenerative amplifier (Alpha-1000S, B. M. Industries) at a 1-kHz repetition rate and had a duration of 80 fs, 12-nJ energy per pulse and a spectrum centered at 800 nm. The other pulse (the idler pulse), being centered at 1100 nm with an 80-fs duration and 48-nJ energy per pulse, was converted from the fundamental pulse by an optical parametric amplifier (COMET-400S, B. M. Industries). That is, the idler pulse was generated by the two-stage parametric amplification of white-light continuum based on a single-filament SPM of the fundamental pulse. Therefore, the carrier phase difference between them was locked [10–12].

The length of the fiber was 3 mm, which almost equals the walk-off length (5 mm) between the two pulses. The delay time of the fundamental pulse with respect to the idler pulse was adjusted by a delay stage with a sub-μm accuracy, and was calibrated by the observation of the sum-frequency light using a 10-μm β-barium borate (BBO) crystal. To focus these two input pulses into the fiber and collimate its output, a pair of nondispersive reflective objectives ($\times 36$) coated with gold and silver, respectively, was used. The typical fiber output efficiency was 20%. The output pulse from the fiber was directed to a pair of prisms with a slit for spectrally resolved measurements of autocorrelation traces, or to a SLM pulse shaper for phase-dispersion compensation. The distance between two fused-silica, 60-degree prisms with double paths was 610 mm. The 4-f pulse shaper consisted of a pair of gratings (with grating constant $d = (1/150)$ mm), a pair of concave mirrors (focal length $f = 350$ mm) and a novel SLM, which was fabricated by one of the authors (A. S.). It has 648 pixels and an 8-bit resolution (a pixel width of 97 μm and a pixel gap of 5 μm). The throughput of the 4-f system was about 30%. After passing the prism pair or the 4-f pulse shaper, the output pulse was characterized by a noncollinear autocorrelator with a 10-μm-thick BBO crystal.

2.2 *Effective discontinuities in group delay and group-delay dispersion*

In our experiment, the fundamental and idler pulses were simultaneously focused into the fiber (with a null delay time). In this case, both dispersive IPM and SPM effects occurred in the fiber, with the spectral broadening from 730 to 1250 nm, as shown in Fig. 2a. First, the corresponding autocorrelation trace (without any chirp compensation) was measured, as depicted in Fig. 2b. The full width at half maximum (FWHM) of the trace is 150 fs.

Second, the autocorrelation trace of the pulse with best phase-dispersion compensation by only a pair of silica prisms was measured, as shown in Fig. 3a. This trace with FWHM of 52 fs was composed of three peaks, which indicated double pulses. To clarify the spectral phase behavior of the pulse, we measured the spectrally resolved autocorrelation traces under prism phase-dispersion compensation [13], as depicted in Fig. 3b,c and d. They correspond to wavelength regions of 730–850, 850–1010 and 1010–1250 nm, and have FWHMs of 55, 40 and 41 fs, respectively. The autocorrelation FWHMs derived from the transform-limited pulse durations of 22 fs are 34 fs for all spectrally resolved regions, on the assump-

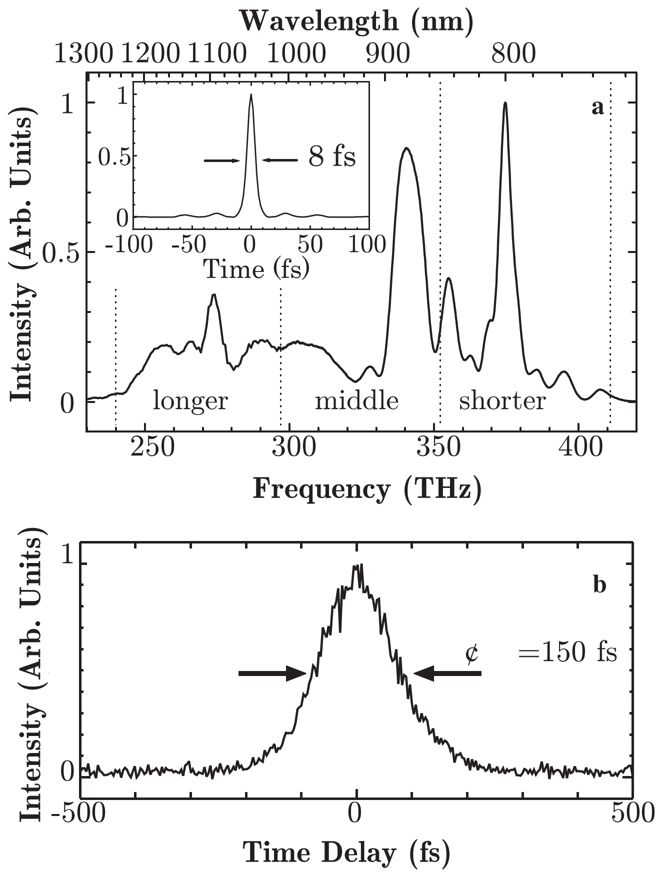

FIGURE 2 **a** Spectrum of the output pulse from the fiber broadened by dispersive induced- and self-phase modulations. The corresponding calculated transform-limited pulse is shown in the *inset*. **b** The corresponding autocorrelation trace of the fiber output pulse without any compensation

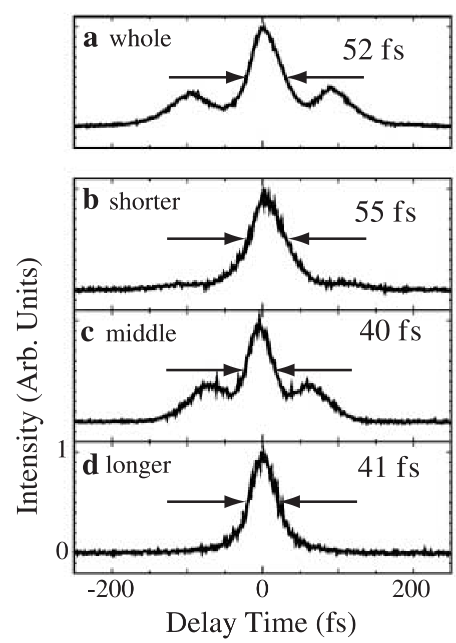

FIGURE 3 Spectrally resolved autocorrelation traces of the pulse whose phase dispersion was compensated for by a prism pair. **a** Whole wavelength region (730–1250 nm), **b** shorter-wavelength region (730–850 nm), **c** middle-wavelength region (850–1010 nm) and **d** longer-wavelength region (1010–1250 nm)

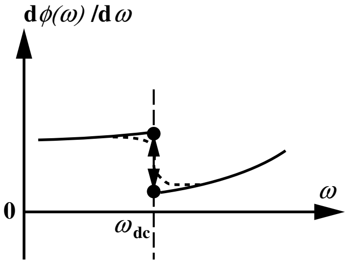

FIGURE 4 Schematic drawing of the pulse group delay $\mathrm{d}\phi(\omega)/\mathrm{d}\omega$. Although, in the strict sense, the spectral phase of the pulse $\phi(\omega)$ may be shown by the *dashed line*, it can be approximately expressed by a combination of two cubic spectral phase functions with respect to ω, as the *solid line*. Group delay as well as group-delay dispersion can be considered to have an effective discontinuity at the frequency ω_{dc} in the middle-wavelength region

tion of sech^2 pulse shapes. The deviations of the measured FWHMs from the transform-limited FWHMs are due to fluctuation in pulse intensity and phase during the accumulation time of 16 s, which is required for low-signal detection. Particularly, the larger deviation in the shorter-wavelength region suggests stronger IPM, which is difficult to compensate for by only a prism pair, originating from higher intensity of idler. In the shorter-wavelength region (b) and the longer-wavelength region (d), phase-dispersion compensation with different prism insertions from each other results in a single-peak autocorrelation trace. In good contrast to this, in the middle-wavelength region (c) the autocorrelation trace has three peaks. In the strict sense, the spectral phase induced- and self-modulation may vary continuously as the dashed line shown in Fig. 4. However, it can be approximately expressed by a combination of cubic spectral phase functions with respect to ω, as the solid line shown in Fig. 4. It is supported by the calculated result from equations describing IPM and SPM nonlinear propagation [2]. Thus the experimental result in the middle-wavelength region suggests the effective discontinuity in group delay (GD) $\mathrm{d}\phi(\omega)/\mathrm{d}\omega$ and the effective discontinuity in group-delay dispersion (GDD) $\mathrm{d}^2\phi(\omega)/\mathrm{d}\omega^2$ expressed by a combination of two functions as the solid line shown in Fig. 4.

2.3 *Phase-dispersion compensation by a SLM*

The chirp compensation implies, in general, that $\mathrm{d}[\phi(\omega)+\phi^{\mathrm{SLM}}(\omega)]/\mathrm{d}\omega = \text{const.}$, where $\phi(\omega)$ and $\phi^{\mathrm{SLM}}(\omega)$ are the spectral phase of pulses and the phase to be applied by a SLM, respectively. However, in the present case of the induced- and self-phase-modulated pulse, unlike the conventional case of the self-phase-modulated pulse, $\mathrm{d}\phi(\omega)/\mathrm{d}\omega$ includes the effective group-delay discontinuity of $\phi'(\omega_{\mathrm{dc}}+0)-\phi'(\omega_{\mathrm{dc}}-0)$ at ω_{dc}, where

$$\phi'(\omega_{\mathrm{dc}}+0) \equiv \lim_{\omega\to\omega_{\mathrm{dc}}+0} \mathrm{d}\phi(\omega)/\mathrm{d}\omega, \tag{1}$$

$$\phi'(\omega_{\mathrm{dc}}-0) \equiv \lim_{\omega\to\omega_{\mathrm{dc}}-0} \mathrm{d}\phi(\omega)/\mathrm{d}\omega, \tag{2}$$

as shown by the solid line in Fig. 4. Therefore, from the experimental result mentioned above, for perfect compensation of the phase dispersion to generate the shortest pulse, the total group delay $t_{\mathrm{d}}^{\mathrm{SLM}}(\omega)$ to be applied by a SLM should be expressed by

$$t_{\mathrm{d}}^{\mathrm{SLM}}(\omega) = \mathrm{d}\phi^{\mathrm{SLM}}(\omega)/\mathrm{d}\omega$$
$$= \begin{cases} C_2^{(1)}(\omega-\omega_{01}) + C_3^{(1)}(\omega-\omega_{01})^2/2, & \omega < \omega_{\mathrm{dc}}, \\ t_{\mathrm{g}} + C_2^{(2)}(\omega-\omega_{02}) + C_3^{(2)}(\omega-\omega_{02})^2/2, & \omega \geq \omega_{\mathrm{dc}}, \end{cases} \tag{3}$$

where ω_{01} and ω_{02} are the center angular frequencies of the Taylor expansion corresponding to 1100 and 800 nm, respectively, and ω_{dc} is the angular frequency where the total group delay $t_{\mathrm{d}}^{\mathrm{SLM}}(\omega)$ is discontinuous. The value of ω_{dc} is determined to be 930 nm from the calculation describing IPM and SPM nonlinear propagation [2, 14]. Parameters $C_2^{(i)}$ and $C_3^{(i)}$ $(i=1,2)$ are the GDD and the third-order dispersion (TOD) in the region of $\omega < \omega_{\mathrm{dc}}$ or $\omega \geq \omega_{\mathrm{dc}}$, respectively. The constant group delay t_{g} is determined so that the discontinuity $\phi'(\omega_{\mathrm{dc}}+0)-\phi'(\omega_{\mathrm{dc}}-0)$ of the group delay vanishes. Figure 5a shows the autocorrelation trace in the case where $C_2^{(1)} = -500\,\mathrm{fs}^2$, $C_3^{(1)} = -200\,\mathrm{fs}^3$, $C_2^{(2)} = -700\,\mathrm{fs}^2$ and $C_3^{(2)} = -700\,\mathrm{fs}^3$ with $t_{\mathrm{g}} = 0\,\mathrm{fs}$ were applied by a SLM in the same manner as in [6–8]. They were determined based on the fact that these values resulted in best chirp compensation when only the fundamental pulse or the idler pulse propagated in the fiber with only the SPM effect. The three-peak trace of Fig. 5a is very similar to that of Fig. 3a, suggesting the effective group-delay discontinuity. To cancel this frequency-independent group-delay effect, we applied the value of t_{g} to be $-120\,\mathrm{fs}$ together with the same $C_2^{(i)}$ and $C_3^{(i)}$ $(i=1,2)$ values and obtained a single-peak autocorrelation trace, as shown in Fig. 5b. The correlation FWHM was 75 fs, which was the same as that of the main peak of Fig. 5a, and the duration of the compensated pulse was evaluated to be 49 fs on the assumption of a sech^2 pulse shape. The corresponding duration of the transform-limited pulse is 8 fs, as shown in the inset of Fig. 2a. The reason for this disagreement is considered to be as follows. In the present experiment, the applied GDD and TOD dispersion parameters using a SLM were determined

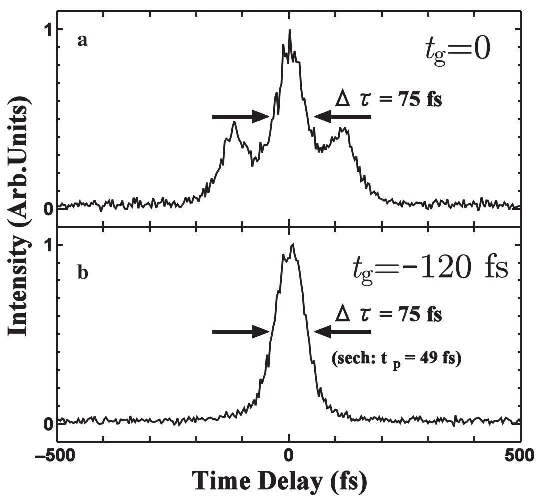

FIGURE 5 Autocorrelation traces of pulses **a** with $C_2^{(1)} = -500\,\mathrm{fs}^2$, $C_3^{(1)} = -200\,\mathrm{fs}^3$, $C_2^{(2)} = -700\,\mathrm{fs}^2$, $C_3^{(2)} = -700\,\mathrm{fs}^3$ and $t_{\mathrm{g}} = 0\,\mathrm{fs}$ (no frequency-independent group-delay adjustment), and **b** with the same parameters as in **a** except that $t_{\mathrm{g}} = -120\,\mathrm{fs}$ (with the frequency-independent group-delay adjustment)

based on the experimental results where only SPM occurred. That is, either the idler or the fundamental pulse propagated in a fiber. Moreover, fluctuation in pulse intensity and phase during a comparable long accumulation time to improve the signal to noise ratio for a low-intensity output from a fiber restricts the resolvable correlation FWHM to be ~ 35 fs.

The optimum value of $t_g = -120$ fs was determined on the basis of the time difference between the main peak and the sub-peak in the autocorrelation trace of Fig. 5a. This group delay is significantly different from the 48-fs propagation time difference of the idler pulse with respect to the fundamental pulse due to the group-velocity difference. Therefore, this result also suggests that the effective group-delay discontinuity originates from the dispersive IPM and SPM effects.

Thus, it should be noted that pulse compression using IPM with two phase-locked optical pulses requires not only conventional nonlinear-chirp compensation but also frequency-independent group-delay adjustment. Both compensations are simultaneously performed by a 4-f system with a SLM. Accurate characterization of the spectral phase using our modified SPIDER technique [15] and better phase-dispersion compensation based on it will enable us to generate much shorter optical pulses such as few-cycle or monocycle pulses.

3 Conclusion

In conclusion, we measured spectrally resolved autocorrelation traces of the ultra-broadband pulse generated by dispersive IPM and SPM. From these measurements, we found effective discontinuities in group delay and group-delay dispersion in the overlapping spectral region of the two input pulses, which were caused by IPM. Moreover, we experimentally demonstrated novel phase-dispersion compensation for the ultra-broadband femtosecond optical pulse generated by dispersive IPM and SPM, using a 4-f optical pulse shaper with a spatial light-phase modulator. In compression of the ultra-broadband optical pulses utilizing the IPM effect with two phase-locked pulses, not only conventional nonlinear-chirp compensation but also frequency-independent group-delay adjustment are essential.

REFERENCES

1 M. Yamashita, H. Sone, R. Morita: Jpn. J. Appl. Phys. **35**, L1194 (1996)
2 M. Yamashita, H. Sone, R. Morita, H. Shigekawa: IEEE J. Quantum Electron. **QE-34**, 2145 (1998)
3 N. Karasawa, R. Morita, L. Xu, H. Shigekawa, M. Yamashita: J. Opt. Soc. Am. B **16**, 662 (1999)
4 L. Xu, N. Karasawa, N. Nakagawa, R. Morita, H. Shigekawa, M. Yamashita: Opt. Commun. **162**, 256 (1999)
5 N. Karasawa, R. Morita, H. Shigekawa, M. Yamashita: Opt. Lett. **25**, 183 (2000)
6 L. Xu, N. Nakagawa, R. Morita, H. Shigekawa, M. Yamashita: IEEE j. Quantum Electron. **QE-36**, 893 (2000)
7 L. Xu, L. Li, N. Nakagawa, R. Morita, M. Yamashita: IEEE Photon. Technol. Lett. **12**, 1540 (2000)
8 N. Karasawa, L. Li, A. Suguro, H. Shigekawa, R. Morita, M. Yamashita: J. Opt. Soc. Am. B **18**, 1742 (2001)
9 L. Li, S. Kusaka, N. Karasawa, R. Morita, H. Shigekawa, M. Yamashita: Jpn. J. Appl. Phys. **40**, L684 (2001)
10 M. Bellini, T.W. Hänsch: Opt. Lett. **15**, 1049 (2000)
11 J.A. Armstrong, N. Bloembergen, J. Ducuing, P.S. Pershan: Phys. Rev. **127**, 1918 (1962)
12 G.D. Boyd, D.A. Kleinman: J. Appl. Phys. **39**, 3597 (1968)
13 M. Hirasawa, N. Nakagawa, M. Shibata, R. Morita, H. Shigekawa, M. Yamashita: Tech. Dig. Conf. Lasers Electro-Opt. (CLEO), Baltimore, Maryland, 2001, p. 270
14 N. Karasawa, S. Nakamura, N. Nakagawa, M. Shibata, R. Morita, H. Shigekawa, M. Yamashita: IEEE J. Quantum Electron. **QE-37**, 398 (2001)
15 M. Hirasawa, N. Nakagawa, K. Yamamoto, R. Morita, H. Shigekawa, M. Yamashita: Tech. Dig. Ultrafast Opt., Montebello, Québec, 2001, p. 241 and Appl. Phys. B. **74** (2002), DOI: 10.1007/s00340-002-0891-y